

# Modeling the Effects of Wind Turbines on Radar Returns

R. Ryan Ohs, Gregory J. Skidmore, Dr. Gary Bedrosian

Remcom, Inc.  
State College, PA USA

**Abstract**— Wind turbines located near radar installations can significantly interfere with a radar’s ability to detect its intended targets. In order to better understand and mitigate the adverse effects of wind turbines on radar, the government and wind farm community need tools that can be used to analyze the radar returns from wind turbines. Remcom’s XGtd<sup>®</sup> software is a high frequency solver capable of calculating the radar cross section of electrically large objects. In this paper, interference from wind turbines is predicted using XGtd simulations and new post-processing algorithms that calculate Doppler shift quantities based on points of interaction with the rotating turbine blades. Results of the analysis are used to calculate the bistatic radar cross section and Doppler shift from two blade orientations. In addition, the time-varying monostatic radar cross section and Doppler shift for a single wind turbine are analyzed and shown to agree well with measured data from actual wind turbines.

**Keywords**—wind turbines, radar, doppler shift, radar cross section

## I. INTRODUCTION

Several studies and reports have documented the adverse effect that wind turbines and wind farms have on radar returns [1-3], including long range radar, air traffic control, and weather radar. Their impact can be summarized by three major effects:

- Large Size: wind turbine heights can reach 198 meters, including max blade height. This results in large radar cross-section, and potential for detection at long ranges.
- Rotational velocity similar to aircraft: with rotor diameters between 40 and 126 meters spinning at 12-34 RPM (typically at the lower end for larger blades), blade tip velocities can exceed 150 Knots, comparable to a slower aircraft such as a Cessna.
- Wind Farm Sizes: with the number and size of farms growing (some now exceed 1,000 turbines), potential radar clutter can be very significant.

As a result of this problem, many wind farm projects are delayed or denied pending long-term assessments of radar impacts [4]. The New York Times recently reported the results of a survey by the American Wind Energy Association (AWEA) indicating that approximately 9,000 megawatts of wind projects were delayed or abandoned in 2009 due to radar concerns by the military and FAA, and that this was nearly equal to the amount of wind capacity actually built that year [5]. Two recent examples include a 130 wind turbine project in Nantucket Sound [6] and a 300-plus wind turbine project in Oregon [7]. As future wind

farm developers attempt to mitigate the problem with new designs, special materials, and relocation of problematic wind turbines, there will be a need for accurate and reliable modeling and simulation of the wind turbine radar returns.

In this paper, we present the results of an effort to develop a new capability to model the impact of wind turbines on radar signals, including the complex and time-varying nature of the impact of spinning turbine blades on radar returns. Our approach builds on Remcom’s existing XGtd<sup>®</sup> software, adding new specialized post-processing capabilities to handle the unique nature of Doppler shift for rotating turbine blades. The study includes analysis of turbine blade materials and the impact of varying blade positions on RCS and Doppler shift, concluding with a comparison between predicted and measured Doppler and RCS for a wind turbine with blades in motion. The ultimate objective is to demonstrate a new capability to accurately model the impact of wind turbines on radar returns.

## II. METHODS

### A. General Modeling Approach: UTD Ray-Tracing

XGtd<sup>®</sup> is a general purpose ray-based software tool capable of analyzing electromagnetic wave propagation in the vicinity of electrically large structures, including aircraft, ships, and motor vehicles. XGtd combines the Uniform Theory of Diffraction (UTD) with ray-tracing algorithms to predict important propagation mechanisms present in high frequency analysis. The ray-tracing is typically performed using a shooting and bouncing technique, in which many rays are first shot from the plane wave or transmitter and allowed to interact with the geometry, before eventually arriving at receiver locations. Based on the ray path interactions, the electric field of the ray path is determined. The electric field contributions for all ray paths reaching a receiver point are combined to calculate output quantities such as received power, time of arrival, impulse response, far-zone antenna gain, etc.

Monostatic and bistatic radar cross section (RCS) calculation can be performed in XGtd by illuminating the geometry with a plane wave and collecting ray paths at locations in the far zone of the geometry. The incoming plane wave source introduces a set of parallel rays into the project that samples the entire geometry. Mathematically, RCS is calculated as

$$RCS = \lim_{r \rightarrow \infty} \left[ 4\pi r^2 \frac{|E_s|^2}{|E_i|^2} \right] \quad (1)$$

where  $E_s$  is the scattered electric field found by summing the contributions of individual ray paths,  $E_i$  is the field incident at the target, and  $r$  is the observation distance from the target. RCS output includes the magnitude and phase values for the co- and cross-polarized field components with respect to the polarization of the incident plane wave.

### B. Modeling the Wind Turbine

XGtd's ray tracing algorithm requires 3D geometry in the form of planar facets. The geometry of the wind turbine used in this analysis was obtained from Google's 3D Warehouse and is based on the Enercon E66 wind turbine. Figure 1 shows a 3D view of the turbine model within XGtd. After importing the CAD model into XGtd, the geometry was simplified by combining smaller facets into larger ones. The geometry of the blades was also separated from the other features. This allowed the blades to be rotated and loaded back into the project so that many different blade orientations could be analyzed. Further, an observation deck was added below the turbine's nacelle in order to model the same wind turbine as considered in [1]. The finished turbine blades, tower, nacelle, and observation deck were composed of 1,169 facets.

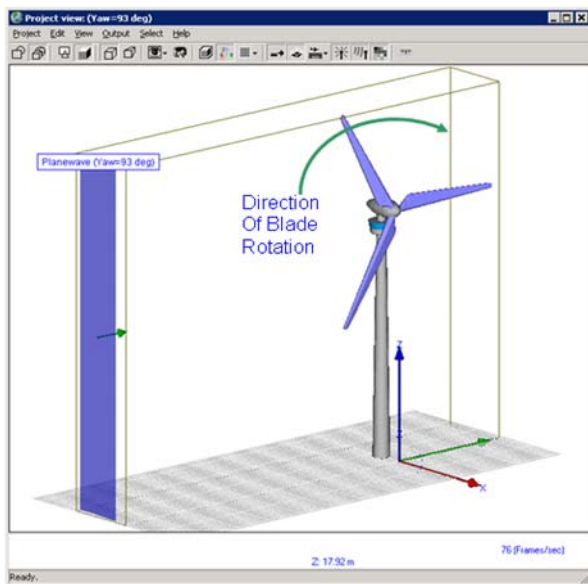


Figure 1: Modeling the Wind Turbine

### C. Material Properties and Thickness of Turbine and Blades

XGtd can model electromagnetic wave interaction with several different material types including perfect electrical conductors (PEC) and layered dielectrics. PEC acts as a perfect reflector and does not allow any transmission. For layered dielectrics, the software calculates the coefficients from each material layer's relative permittivity ( $\epsilon_r$ ), conductivity ( $\sigma$ ), and thickness ( $t$ ). These material types can be separately defined for each facet in the project geometry, and are used to calculate the reflection, diffraction and transmission coefficients, which determine the effect on the electric field of each ray path that interacts with a facet.

In this study, three materials were used in the model of the wind turbine:

- Perfect electrical conductor for the tower and nacelle
- Glass for the windows of the observation deck ( $\epsilon_r=2.4$ ,  $\sigma=0.0$  S/m,  $t=0.003$  m)
- Fiberglass for the turbine blades ( $\epsilon_r=4.34$ ,  $\sigma=0.0031$  S/m,  $t=0.076$  m)

Generally, modern turbine blades like those used on the Enercon E66 are constructed from hollow shells of composite materials, such as fiberglass. Thickness varies along the blade and depends on the blade size and specific underlying support structure. Although we were unable to determine the precise thickness of the blades of the Enercon E66, an online search reveals that blade thickness on the order of several centimeters (e.g., 10 cm) [8] is not uncommon. For this study, Remcom chose an arbitrary thickness of 7.6 cm (3 inches).

We then performed a sensitivity study to analyze the variation in the reflection coefficient for a single layer of fiberglass as a function of angle and thickness. Figure 2 shows the reflection coefficient, expressed in dB, for fiberglass versus incident angle as a function of blade thickness for a 3 GHz transmitter. This analysis shows substantial variation with thickness, suggesting that proper selection of the blade material thickness may have a significant impact on RCS predictions. Although a specific study was not performed on material properties, we anticipate that these will also play an important role in the calculation of the reflected field magnitude.

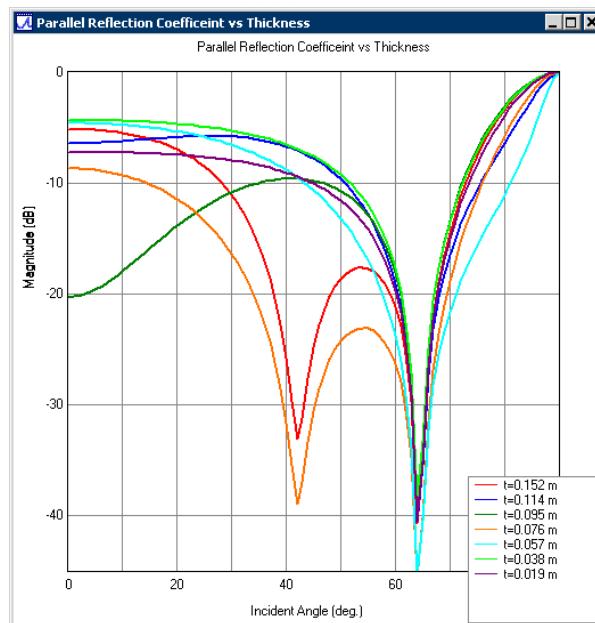


Figure 2: Reflection Varies with Blade Shell Thickness

### D. Doppler Shift for Rotating Blades

In a ray-tracing approach, the returned fields at a radar will equal the sum of fields returned from all paths to the wind turbine and back. To first order, each path that scatters

from one or more points on the moving turbine blades can be considered to have a discrete Doppler shift that is related to the point or points where it reflects or diffracts from the turbine blade. A sequential set of rays that samples along the surface of the turbine blade will then capture the spread of Doppler shift from the rotor hub to the blade tips.

For any given propagation path, there may be several points of interaction with the wind turbine, including multiple reflections and diffractions from the tower or nacelle, turbine blades, and in more complex scenes, additional turbines, buildings or ground. For a propagation path that has  $N$  interactions, the total Doppler shift can be calculated as follows:

$$\Delta f = \sum_{i=1}^{N+1} \frac{\vec{u}_i \cdot (\vec{v}_i - \vec{v}_{i-1})}{\lambda_0} \text{ Hz} \quad (2)$$

where  $\vec{u}_i$  is the unit vector direction of the propagating wave at each interaction point, and  $\vec{v}_i$  is the velocity of the transmitter, object interacted with, or receiver, at each interaction point. For a scattering point on a rotating blade, the velocity at the interaction point is calculated by

$$\vec{v}_i = \vec{\omega} \times \vec{r}_i \quad (3)$$

where  $\vec{\omega}$  is the rotational velocity vector of the turbine and  $\vec{r}_i$  is the vector from the center of rotation to the interaction point.

In actuality, because the Doppler shift for a Radar is several orders of magnitude lower than the carrier frequency, most Doppler radars do not calculate the Doppler shift directly from a single pulse. Instead, they use a technique that employs two pulses and determines the phase shift between them. Through a similar set of equations to (1) and (2), the total rate of change of the path length can be calculated, and from that the phase shift can be determined. If two radar pulses are separated in time by  $\Delta t$  and the path length for a given path is changing at a rate of  $dD/dt$ , the phase shift between them, in radians, is given by

$$\Delta\phi = \frac{2\pi}{\lambda} \frac{dD}{dt} \Delta t \quad (3)$$

where  $\lambda$  is the wavelength of the carrier frequency.

In this study, Remcom prototyped both sets of equations and used them in post-processing analysis to predict the effect of the blade rotation on radar returns. The results in this paper focus on the Doppler shift.

### III. RESULTS

Using the model of the Enercon E66 turbine, RCS calculations were made by illuminating the wind turbine with a plane wave from the side. This represents the worst case for the Doppler shift because in the positive or negative vertical direction (the orientations with peak RCS), the velocity vector is either equal to or opposite the direction of the plane wave. In the first phase of analysis, the blades were assessed without the nacelle and tower, in order to demonstrate the ability of the approach to generate Doppler

shift information from the ray path data. This included both the RCS and Doppler shift resulting from interaction with the blades. Two cases were considered: a worst-case orientation with one of the blades in the vertical position, and a low-backscatter case with one blade tip pointed at the radar and the other two blades oriented away (see blade positions in the top-left diagrams of Figure 3 and Figure 4).

Next, the RCS was predicted in the return direction as a function of time for one complete rotation of the turbine blades, including interactions with the full geometry of the wind turbine (blades, nacelle, and tower). By sequentially simulating 360 different blade orientations, a plot of the RCS and Doppler shift vs. time for the wind turbine was generated.

#### A. Radar Cross Section of Turbine Blades

Beginning with the blade-only analysis, the XGtd-based simulation approach was first used to calculate the radar cross section for the two aforementioned orientations. This analysis used an incident plane wave with a frequency of 1.3 GHz. The bistatic scattering in the plane of the turbine blades are presented in Figure 3 for Case 1 and in Figure 4 for Case 2.

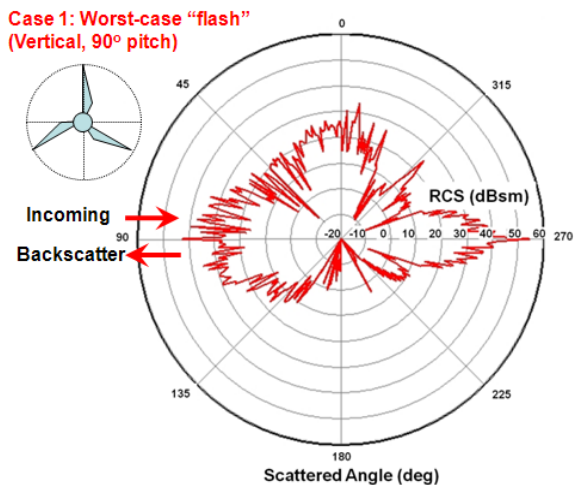


Figure 3: Turbine Blade RCS Case1: Worst-Case Flash.

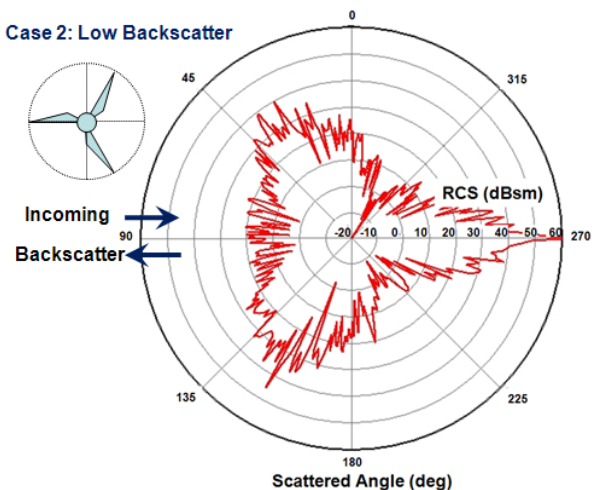


Figure 4: Turbine Blade RCS Case2: Low Backscatter

### B. Doppler Shift Due to Turbine Blade Rotation

During the ray tracing, XGtd stores the location that each ray interacts with the blade geometry. From the ray path data, it is possible to determine which facet the ray interacted with, the angle of incidence the ray approached from, and the departure angle of the ray. By locating the facet on the geometry, the velocity vector of the facet can be calculated. These values can then be used in equation (2) to determine the Doppler shift of each ray path.

Figure 5 shows the Doppler shift associated with each ray path that reached the backscatter direction for Case 1 and Case 2. The blades in both cases were rotating at a constant speed of 16 rpm. The Doppler shifts for Case 1 clearly show the impact of the vertical blade moving towards the plane wave. Here most of the ray paths experience a positive Doppler shift. The Doppler shifts for Case 2 are more evenly distributed due to the symmetric orientation of the upper blade which is moving towards the plane wave and the lower blade which is moving away from the plane wave.

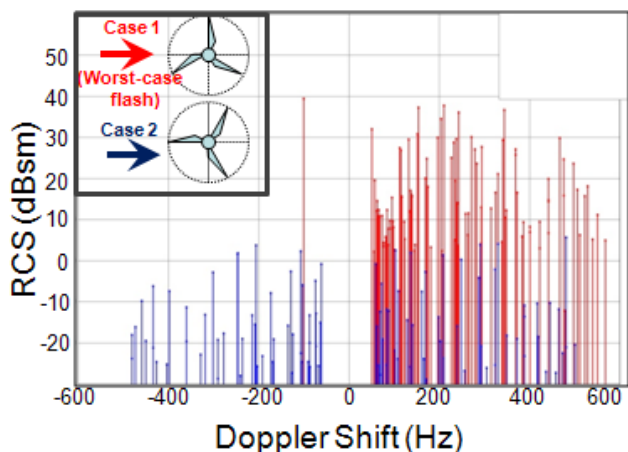


Figure 5: Doppler Shift for Case1 (red) & Case 2 (blue)

### C. RCS and Doppler Shift of a Wind Turbine

Next, the entire wind turbine geometry was considered, including the tower and observation deck, the nacelle, and the blades. RCS calculations were run for 120 blade positions ( $1^\circ$  spacing) to represent the turbine rotating a third of one full rotation. The frequency of the incident plane wave was 3 GHz. The ray paths from each simulation were analyzed to determine if they interacted with a moving facet of the wind turbine. In cases where the incident facet was moving, the associated Doppler shift was calculated. The RCS contributions of the ray path were then binned by the Doppler shift. Assuming the blades to be rotating at 23 rpm, a corresponding time was calculated for each angular position. The results are presented in Figure 6.

## IV. DISCUSSION

In the blade RCS analysis, the first case considered the top turbine blade to be vertical and moving towards the incoming plane wave. This would represent the worst case in terms of RCS scattering and Doppler shift. The entire length of the vertically oriented blade would be visible and

the velocity vector of the blade would be in the opposite direction of the plane wave. Figure 3 shows the bistatic RCS in the same plane as the turbine blades. Note that in this figure, the blades would be rotating in the counter-clockwise direction.  $0^\circ$  represents the upwards direction,  $90^\circ$  is the direction of the approaching plane wave and is also the angle of the backscatter.  $180^\circ$  represents the forward scatter direction, and  $270^\circ$  is towards the ground. Figure 3 shows a backscatter RCS of 43 dBsm.

The second case considered the situation when one blade points directly towards in the incoming plane wave. Here the plane wave is only incident on the tip of one blade and the other two blades tend to scatter the incoming energy off along  $30^\circ$  and  $150^\circ$ . Simulation results show RCS in the backscatter direction to be about 20 dBsm, which is approximately 23 dBsm less than the backscatter in case 1. The values for RCS in the backscatter direction for Case 1 and Case 2 are consistent with the range of RCS values commonly reported from large wind turbines [1, 2].

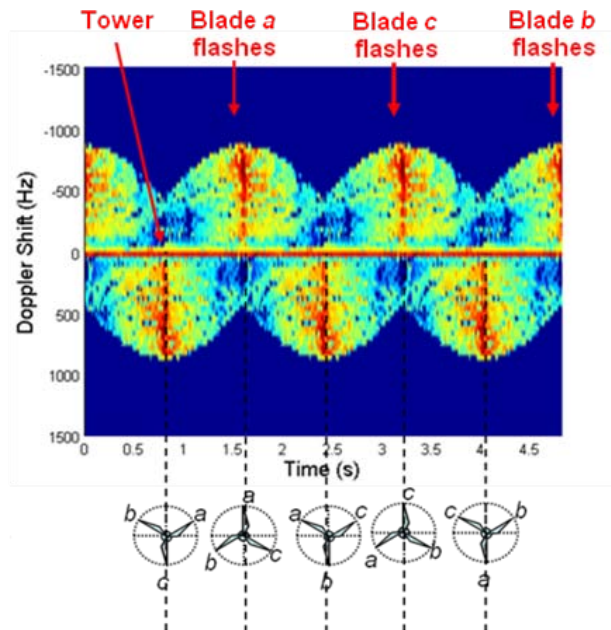
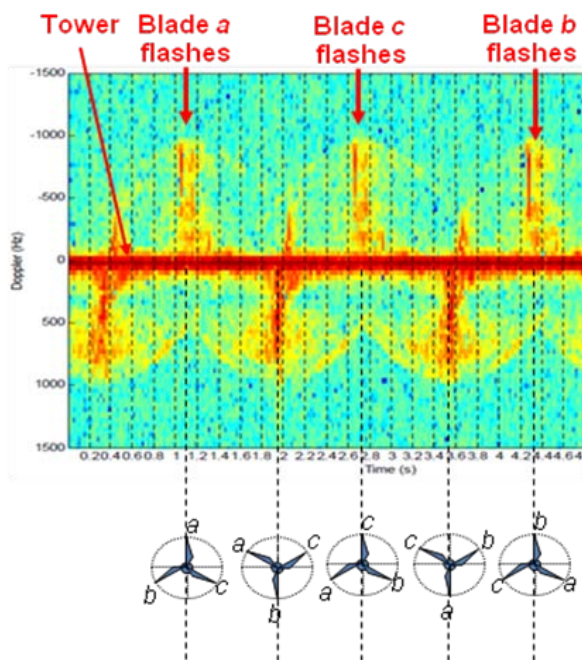


Figure 6: What a Radar Sees: RCS & Doppler vs. Time

In the full wind turbine geometry analysis, after the results are assembled in the time domain, the unique contributions of each blade can be clearly seen as the turbine rotates. As each blade reaches a vertical position, there is a clear RCS flash on the diagram. When the blade is pointed upwards, the flash is associated with a negative Doppler shift as the upper part of the blade moves away from the radar location. A large positive Doppler shift is present when the blades are pointed downwards and moving towards the radar location. The magnitudes of the peak Doppler shifts are consistent with the rotational velocity of the turbine. Also present in Figure 6 is a strong RCS magnitude occurring at zero Doppler shift. This represents the RCS contribution from rays interacting with the stationary components of the wind turbine such as the tower, observation deck and rear part of the nacelle. The behavior

and values of the calculations presented in Figure 6 are in good agreement with measured data shown in Figure 7, which were obtained from a single wind turbine located in Swaffham, UK[1].



**Figure 7: Measured Data: RCS & Doppler vs. Time**  
(Underlying Doppler/RCS Image is from ref. [1])

## V. FUTURE DIRECTIONS

The single wind turbine near Swaffham, UK is a rather rare instance. Most wind turbines are being grouped into wind farms that contain several hundred turbines. This can greatly complicate simulation of the problem as energy can scatter deep into the wind farm and return back to the radar. Nearby buildings and terrain features can also serve to further complicate the analysis. Remcom is currently working on algorithms and approaches to simulate key interactions that occur when several turbines are located near one another as would be the case for large wind farm scenarios (see Figure 8).

## VI. CONCLUSION

Returns from the rotation of wind turbine blades can interfere with neighboring radars and produce images that can be confused for moving aircraft or conceal actual approaching aircraft. As wind farms are more frequently being built near radars, it is becoming increasingly important to understand the effects the wind turbines have on radar performance. For this study, Remcom's high frequency solver, XGtd, was used to analyze the radar cross section of a wind turbine. XGtd is particularly well suited for this problem because its calculations include the effects of material properties and turbine geometry, both of which are key elements in some of the solutions that have been proposed to the wind turbine interference problem. To capture the Doppler shift and time-varying nature of wind turbine scattering effects, new post-processing algorithms were developed. These take advantage of information

provided by the XGtd ray-based solver regarding the locations where rays interact with the project geometry, and combine this information with local velocities based on distance from the axis of rotation in order to calculate a Doppler shift for each ray path.

The bistatic radar cross section of two blade orientations showed good qualitative agreement with values published in the literature. Analysis of the monostatic radar cross section binned by Doppler shift, and simulated over several seconds of turbine blade rotation matched well with a similar diagram that was generated from measurements. These examples demonstrate that the approach, based on the ray-based XGtd solver enhanced with new post-processing algorithms for rotational velocity and Doppler shift, can be used to effectively evaluate the radar return from a wind turbine.

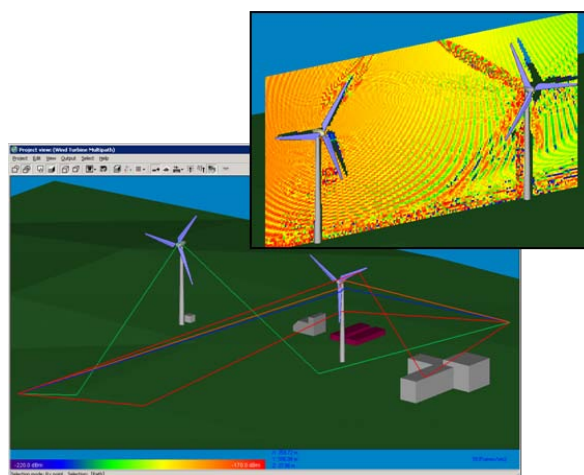


**Figure 8: Future Work: Investigate Multipath Effects**  
(Multipath Modeling in Wireless InSite®)

## REFERENCES

1. G. J. Poupart, "Wind farms Impact on radar aviation interests – Final report," DTI PUB URN 03/1294, prepared by QinetiQ for Department of Trade and Industry (DTI), September 2003.
2. B. M. Kent, K. C. Hill, A. Buterba, G. Zelinski, R. Hawley, & et al, "Commercial general electric windmill power turbines part 1: Predicted and measured radar signatures," IEEE Antennas and Propagation Magazine, vol 50 (2), pp. 211-219, April 2008.
3. R. J. Vogt, T. D. Crum, J. B. Sandifer, E. J. Ciardi, and R. Guenther, "A Way Forward; Wind Farm – Weather Radar Coexistence," NOAA NEXRAD Radar Operations Center report, [http://www.rost.noaa.gov/WSR88D/Publicdocs/WindPower2009\\_Final.pdf](http://www.rost.noaa.gov/WSR88D/Publicdocs/WindPower2009_Final.pdf).
4. M. Brenner, "Wind Farms and Radar," JSR-08-126 prepared by The Mitre Corporation, January 2008.
5. L. Vestel, "Wind Turbine Projects Run into Resistance," New York Times, August 25, 2010, <http://www.nytimes.com/2010/08/27/business/energy-environment/27radar.html>.
6. M. Finucane, "FAA finds Cape Wind project would cause radar interference," The Boston Globe, February 13, 2009, [www.boston.com](http://www.boston.com).
7. S. Learn, "Air Force concerns about radar interference stall huge Oregon wind energy farm," April 14 2010, [www.oregonlive.com](http://www.oregonlive.com).
8. G. Gardiner, "Wind Blade Manufacturing, Part II: Are thermoplastic composites the future?," High Performance Composites Magazine, November 2008, <http://www.compositesworld.com>.